

University of Mississippi

eGrove

---

Honors Theses

Honors College (Sally McDonnell Barksdale  
Honors College)

---

Spring 5-10-2024

## Structural and blood co-factor binding studies of a red algal sulfated galactan

Anderson R. DeWitt  
*University of Mississippi*

Follow this and additional works at: [https://egrove.olemiss.edu/hon\\_thesis](https://egrove.olemiss.edu/hon_thesis)



Part of the [Pharmacy and Pharmaceutical Sciences Commons](#)

---

### Recommended Citation

DeWitt, Anderson R., "Structural and blood co-factor binding studies of a red algal sulfated galactan" (2024). *Honors Theses*. 3160.

[https://egrove.olemiss.edu/hon\\_thesis/3160](https://egrove.olemiss.edu/hon_thesis/3160)

This Undergraduate Thesis is brought to you for free and open access by the Honors College (Sally McDonnell Barksdale Honors College) at eGrove. It has been accepted for inclusion in Honors Theses by an authorized administrator of eGrove. For more information, please contact [egrove@olemiss.edu](mailto:egrove@olemiss.edu).

STRUCTURAL AND BLOOD CO-FACTOR BINDING STUDIES OF A RED ALGAL  
SULFATED GALACTAN

by

Anderson DeWitt

A thesis submitted to the faculty of the University of Mississippi in partial fulfillment of the  
requirements of the Sally McDonnell Barksdale Honors College

Oxford, MS  
May, 2024

Approved by

---

Advisor: Professor Vitor Pomin

---

Reader: Professor Paul Boudreau

---

Reader: Professor Kristine Willett

© 2024  
Anderson DeWitt  
ALL RIGHTS RESERVED

## ACKNOWLEDGEMENTS

I would like to offer thanks to everyone that aided in the process and mentored me throughout the completion of my honors thesis. First, I would like to thank the members of my lab: Dr. Vitor Pomin, Dr. Antim Maura, Marwa Mohammed, Hoda Ahmed, and Chakiya Smith. With your knowledge and willingness to teach me, I was able to learn the importance of research as well as the skill of writing scientifically in preparation for this thesis.

I would also like to express gratitude for the members of the committee as well: Dr. Vitor Pomin, Dr. Paul Boudreau, and Dr. Kristine Willett. Your participation in this project is essential for its success. With you all, the completion and defense of my thesis is possible. Thank you again for your support.

Lastly, I would like to express my thanks for the support of my family and friends. Continual support from my family and belief from my peers allowed me to be disciplined and continue to conduct meaningful research in hopes of completing a thesis. Thank you to everyone for your support and enabling to complete this project which begins many more years of research to come.

## ABSTRACT

ANDERSON DEWITT: Structural and blood co-factor binding studies of a red algal sulfated galactan  
(Under the direction of Vitor H. Pomin)

The red alga *Botryocladia occidentalis* presents three distinct fractions of sulfated polysaccharides. The elucidation of structures of various *B. occidentalis* fractions has been explored in prior research. In this study, the first fraction with the least sulfation underwent NMR structure elucidation. Additionally, this sulfated polysaccharide underwent analysis following chemical modifications. Findings have unveiled the presence of both 4-linked  $\alpha$ - and 3-linked  $\beta$ -galactose units with the following chemical characteristics: over half of the total galactose units are unsulfated, the  $\alpha$ -units are primarily 3,6-anhydrogalactose units either 2-O-methylated or 2-O-sulfated, and the  $\beta$ -galactose units can be 4-O-sulfated or 2,4-O-disulfated. Results from SPR-based assays demonstrated stronger binding of the least sulfated galactan to heparin cofactor II, yet weaker binding to thrombin, factor Xa, and antithrombin compared to unfractionated heparin. This study, combined with our previous publication, concludes the structural characterization of the three polysaccharides present in the cell wall of *B. occidentalis* and elucidates the relationship between their constituent chemical groups and their interactions with blood co-factors.

## TABLE OF CONTENTS

|   |            |
|---|------------|
| <b>LIST OF FIGURES/TABLES</b> .....                                       | <b>vi</b>  |
| <b>LIST OF ABBREVIATIONS</b> .....  | <b>vii</b> |
| <b>1. Introduction</b> .....  | <b>1</b>   |
| 1.1 Sulfated polysaccharides.....   | 2          |
| 1.2 <i>Botryocladia occidentalis</i> .....                                | 3          |
| 1.3 NMR spectroscopy in structural elucidation .....                      | 3          |
| 1.4 SPR spectroscopy in binding analyses.....                             | 4          |
| <b>2. Methods</b> .....   | <b>5</b>   |
| 2.1 Digestion of <i>B. occidentalis</i> sulfated galactan (BoSG).....     | 5          |
| 2.2 Anion-exchange chromatography.....                                    | 6          |
| 2.3 1,9-dimethylmethylene blue (DMB) .....                                | 6          |
| 2.4 Polyacrylamide gel electrophoresis (PAGE) .....                       | 7          |
| 2.5 Chemical modifications of BoSG .....                                  | 7          |
| 2.5.1 Desulfation of BoSG Fr1.....  | 7          |
| 2.5.2 Oversulfation of BoSG Fr1.....                                      | 8          |
| 2.5.3 Alkaline treatment of BoSG Fr1 .....                                | 8          |
| <b>3. Results and Discussion</b> .....                                    | <b>9</b>   |
| 3.1 Structure characterization of BoSG.....                               | 9          |
| 3.1.1 Isolation and preliminary physiochemical analyses of BoSG Fr1 ..... | 9          |
| 3.1.2 NMR spectroscopy .....  | 11         |
| 3.2 Binding properties of BoSG Fr1 .....                                  | 17         |
| 3.2.1 SPR spectroscopy .....  | 17         |
| <b>4. Conclusions</b> .....   | <b>19</b>  |
| <b>REFERENCES</b> .....   | <b>21</b>  |

## LIST OF FIGURES/TABLES

|   |           |
|---|-----------|
| <b>Figure 1.</b> Image of <i>Botryocladia occidentalis</i> .....  | <b>3</b>  |
| <b>Figure 2.</b> Fractionation of BoSG.....   | <b>10</b> |
| <b>Figure 3.</b> HPSEC-MALS profile of BoSG Fr1 .....   | <b>11</b> |
| <b>Figure 4.</b> PAGE MW analysis of BoSG Fr1 .....   | <b>11</b> |
| <b>Figure 5.</b> 1D <sup>1</sup> H NMR spectrum of BoSG Fr1 ( $\delta_H$ expansion from 6.0 to 3.0 ppm).....  | <b>12</b> |
| <b>Figure 6.</b> 2D NMR spectra of BoSG Fr1 [A,B,C]. .....  | <b>13</b> |
| <b>Table 1.</b> <sup>1</sup> H and <sup>13</sup> C chemical shifts (ppm) <sup>a</sup> of the composing units from BoSG Fr1.....                                 | <b>14</b> |
| <b>Figure 7.</b> 2D NMR spectra of BoSG Fr1 chemical derivatives [A,B,C] .....  | <b>16</b> |
| <b>Figure 8.</b> Structural illustration of BoSG Fr1. ....  | <b>17</b> |
| <b>Figure 9.</b> Solution SPR competitive effects of native BoSG and its chemical derivatives on binding of blood co-factors to heparin surface [A,B,C,D] ..... | <b>19</b> |

## LIST OF ABBREVIATIONS

|  |   |
|--|---|
| 1,9-dimethylmethylene blue<br>(DMB)  | Heparin cofactor II<br>(HCII)                             |
| $^1\text{H}/^{13}\text{C}$ -edited heteronuclear single quantum<br>coherence<br>(HSQC) | High performance size-exclusion chromatography<br>(HPSEC) |
| $^1\text{H}/^1\text{H}$ correlation spectroscopy<br>(COSY)                             | Low molecular weight heparin<br>(LMWH)                    |
| $^1\text{H}/^1\text{H}$ total correlation spectroscopy<br>(TOCSY)                      | Methoxy group<br>(O-CH <sub>3</sub> )                     |
| 3,6-anhydrogalactose<br>(AnGal)  | Molecular weight<br>(MW)                                  |
| Alkali-treated<br>(AnGal-enriched)   | Multi-angle light scattering<br>(MALS)                    |
| Antithrombin<br>(AT)   | Nuclear magnetic resonance<br>(NMR)                       |
| Botryocladia occidentalis<br>( <i>B. occidentalis</i> )                                | Polyacrylamide gel electrophoresis<br>(PAGE)              |
| Botryocladia occidentalis sulfated galactan<br>(BoSG)                                  | Sodium acetate<br>(NaOAc)                                 |
| Cetylpyridinium chloride solution<br>(CPC)   | Sodium chloride<br>(NaCl)                                 |
| Chondroitin sulfate A<br>(CS-A)  | Sulfated galactans<br>(SGs)                               |
| Chondroitin sulfate C<br>(CS-C)  | Surface plasmon resonance<br>(SPR)                        |
| Dimethyl sulfoxide<br>(DMSO)   | Thrombin<br>(IIa)   |
| Ethylenediaminetetraacetic acid<br>(EDTA)  | Two-dimensional<br>(2D)                                   |
| Galactose<br>(Gal)   | Unfractionated heparin<br>(UFH)                           |

## 1. Introduction

Medically relevant compounds can be found in populations of marine organisms [1]. Sulfated polysaccharides from marine algae have been shown to provide an assortment of potential therapeutic properties [2]. The type of polysaccharide found in the cell walls of red algae are sulfated galactans (SGs). The SGs in this paper are found as 3-linked beta-D-galactose (Gal) and 4-linked alpha-L/D-Gal units sulfated with a molecular weight (MW) more than 100 kDa. The D configuration of an algal SG classifies it as a carrageenan while the L configuration classifies it as an agaran [2]. Variations in the algal SGs can also occur as 3,6-anhydrogalactose (AnGal) units in the backbone and hydroxyl substitutions through methylation, acetylation, and pyruvylation [2]. Because of the complexity of these compounds, algal SGs provide a researchable topic with many different medicinal applications. Specifically, the use of algal SGs as an anticoagulant drug are one of the most studied applications of these glycans [3].

*Botryocladia occidentalis*, a red alga from the Rhodymeniacea family is one of the most studied seaweeds in reference its structure and biological activity [2]. In the original investigation of the structure of *B. occidentalis* cell wall glycans taking place over two decades ago, three fractions of sulfated polysaccharides from this red alga were isolated [4]. *B. occidentalis* sulfated galactan (BoSG) was also classified as a group of carrageenans [2]. Recent publications have revised the structure of two fractions of *B. occidentalis*; however, little attention was given to the least sulfated BoSG fraction [5].

In this work, BoSG was isolated from the cell wall of *B. occidentalis* with multiple physicochemical analysis performed on the least sulfated BoSG fraction. One-dimensional (1D) and two-dimensional (2D) nuclear magnetic resonance (NMR) spectroscopy, high performance size-exclusion chromatography/multi-angle light scattering (HPSEC/MALS), polyacrylamide gel

electrophoresis (PAGE), and surface plasmon resonance (SPR) spectroscopy were all performed. The 2D NMR methods were  $^1\text{H}/^1\text{H}$  correlation spectroscopy (COSY),  $^1\text{H}/^1\text{H}$  total correlation spectroscopy (TOCSY), and  $^1\text{H}/^{13}\text{C}$ -edited heteronuclear single quantum coherence (HSQC) spectra. To aid in structural identification, chemically modified versions such as desulfated, oversulfated, and alkali-treated (AnGal-enriched) derivatives were utilized for the least sulfated BoSG fraction. Using a heparin surface, SPR analyses were analyzed against the main binding co-factors: thrombin (IIa), factor Xa, antithrombin (AT), and heparin cofactor II (HCII). With previous publications and work this work has completed the structural characterization and bioactivity evaluation of all three BoSGs.

### **1.1 Sulfated polysaccharides**

Sulfated polysaccharides are complex anionic carbohydrates that consist of sulfate groups attached to sugar units of the molecule [6]. Abundantly found in natural sources, sulfated polysaccharides appear in marine algae, animal tissues, and microbes [6]. This type of molecule exhibits a multitude of biological activities [6]. Sulfated polysaccharides are reported to exhibit a wide range of roles such as a reported immunomodulator, anti-inflammatory compound, antiviral agent, and anticoagulant [6]. Sulfated polysaccharides appear as great candidates for research and application because of their biocompatibility.

Polysaccharides are composed of simple sugars joined by glycosidic bonds [7]. The anionic charge of sulfated polysaccharides is due to their substituent sulfate groups. Previous research has shown the sulfation of the polysaccharides can result in favorable biological activity [5]. *B. occidentalis* contains specific sulfated polysaccharides which consist of repeated disaccharides linked by glycosidic bonds [5]. The type of glycosidic linkages that compose the polysaccharide found in this red alga classify the polysaccharides as sulfated galactans.

## 1.2 *Botryocladia occidentalis*

*B. occidentalis* is a species of red algae commonly known as “West Indian Plocamium” or “Botryocladia seaweed”. Found in tropical and subtropical regions of the Atlantic Ocean, this alga particularly resides along the western coasts of the Caribbean Sea as well as the Gulf of Mexico and Florida [5]. Three populations of the cell wall from *B. occidentalis* have been isolated by anion-exchange chromatography [5]. The two more sulfated BoSG fractions have been revised by previous research [5]. Figure 1 contains a picture of the red alga *B. occidentalis*.



**Figure 1.** Image of *B. occidentalis*

## 1.3 NMR spectroscopy in structural elucidation

Nuclear Magnetic Resonance spectroscopy is an analytical technique to determine the structure and interactions of molecules. Particularly used with organic compounds, the function of NMR relies on the interaction of atomic nuclei with an external magnetic field and radiofrequency radiation to provide the chemical environment of atoms within a molecule [8]. To construct data to determine the structure and interactions of molecules, NMR utilizes atomic

nuclei with an odd number of protons or neutrons such as  $^1\text{H}$ ,  $^{13}\text{C}$ ,  $^{15}\text{N}$ . When placed in the magnetic field, these nuclei align to produce two energy states [8]. The application of radiofrequency radiation at appropriate frequencies allows the nuclei to transition between these two energy states [9]. The resonance frequency by which the transition between the two states occurs is unique to the chemical environment of the nuclei, which provides information about its surroundings [10].

The resonance frequency observed in NMR spectroscopy is noted as a chemical shift [10]. The chemical shift can vary due to the electron density around the nucleus [8]. Factors affecting electron density include electronegativity, functional groups, and molecular conformation [10]. These factors that affect electron density are structural in nature, thus providing essential information about the composition of compounds [10].

NMR spectroscopy can also provide information about spin-spin coupling, this magnetic interaction appears between neighboring nuclei with non-zero nuclear spin [9]. This allows NMR to provide information about the number, relative position, and the connectivity of adjacent nuclei and atoms within a molecule [8,9,10].

Because NMR spectroscopy can provide information to the connectivity, stereochemistry, and conformation of organic molecules, it is an essential tool for structure elucidation.

#### **1.4 SPR spectroscopy in binding analyses**

Surface Plasmon Resonance (SPR) spectroscopy is another analytical technique to analyze real-time biomolecular interactions between molecules. It is used to provide information about kinetics, affinity, and specificity of the molecular binding [11]. SPR occurs when light interacts with metal at the resonance angle, and this phenomenon excites surface plasmons

leading to a decrease in the reflected light [11]. Because of the sensitivity of the resonance angle to the refractive index of the medium, this technique can be used for studying bioactivity specifically antigen-antibody interactions [12].

To test interactions, an interacting molecule is coupled to the sensor surface. This molecule known as the ligand is immobilized onto the sensor surface. Then another molecule in solution, the analyte, is moved across the immobilized ligand [13]. When the analyte binds to the ligand, it will cause a change in the local refractive index in the gold sensor surface. [13] This binding will result in a shift in the resonance angle and can be interpreted into numerical data. [13]. Because of these changes, binding kinetics and affinity can be determined with the SPR technique due to the principle of surface plasmon resonance.

The SPR analysis is important in determining the activity of a molecule [11]. Specifically for sulfated polysaccharides, surface plasmon resonance spectroscopy can determine the bioactivity of these complex carbohydrates regarding their activities as anticoagulants, antivirals, immunomodulators, and anti-inflammatory agents [5].

## **2. Methods**

### **2.1 Digestion of *B. occidentalis* sulfated galactan (BoSG)**

*B. occidentalis*, the marine red algae, was obtained from Gulf Coast Ecosystems. Following a procedure from the previous paper dealing with structure elucidation of *B. occidentalis* with slight variation, the BoSGs were extracted [5]. The marine red alga was finely chopped, freeze dried, and then lyophilized for 24 h. Then, papain (1 mg papain/g dry tissue), 5 mM ethylenediaminetetraacetic acid (EDTA), and 5 mM cysteine dissolved in 0.1 M sodium acetate (NaOAc) buffer was added to the resulting dried sample (2.5 g) for 24 h at 60 °C. The

incubated mixture was then centrifuged for 30 min at 3000 rpm and the supernatant was collected. This crude polysaccharide solution was then precipitated with 3 mL of 10% cetylpyridinium chloride solution (CPC) and remained at room temperature for 24 h. After obtaining and centrifuging the precipitate for 30 min at 3000 rpm, the mixture was washed with 300 mL of 5% CPC solution. Subjecting the sample to another centrifugation, the polysaccharide was dissolved in 86 mL of 2 M sodium chloride (NaCl) and 15% ethanol solution for incubation at -20 °C for 24 h. Following the centrifugation parameters above, the polysaccharides were recovered and washed twice with 150 mL of 80% ethanol following another wash with 150 mL of absolute ethanol. The resulting precipitate underwent lyophilization for 24 h, yielding the crude polysaccharide which was then stored at 4 °C.

## **2.2 Anion-exchange chromatography**

Fractionation of BoSGs (50 mg) began with the dissolution of crude BoSG from digestion in 1 mL NaOAc (50 mM) buffer. Subsequent purification occurred with a DEAE Sephacel anion-exchange resin column (2.5 x 20 cm). Isolation was performed by gradually increasing NaCl concentration (in 50 mM NaOAc, pH 6.0) from 0 to 3 M at a flow rate of 21 mL/h. The desired BoSG Fr1 fractions (3.5 mL/tube) were set in 6 mL culture tubes. NaCl concentration was determined by conductivity experiments.

## **2.3 1,9-dimethylmethylene blue (DMB)**

Isolation of the desired fraction of BoSG proceeds following the extraction by anion-exchange chromatography. In a 96 well plate, 5 µL of polysaccharide fractions were added from the culture tubes with the 96<sup>th</sup> well containing the buffer which served as the blank. The polysaccharide fractions were mixed in the well plate with 190 µL of the 1,9-dimethylene blue solution. Determination of the polysaccharide fractions were achieved with DMB-based

colorimetric assay. At 525 nm, the absorbance was recorded on a microplate reader (SpectraMax ABS). Based on previous literature of Fr2 and Fr3, we determined that our desired BoSG Fr1, was contained in the tubes preceding the elution of Fr2 in the chromatogram [5]. We determined that our desired BoSG Fr1 was obtained in tubes 40-55 from the Anion Exchange Chromatography. This was confirmed with the DMB-based colorimetric assay in comparison to Fr2 and Fr3 from previous literature [5]. Specific fractions underwent combination, dialysis against distilled water, freeze-drying, and lyophilization. This procedure was repeated eight times to yield a total output of 20 mg for BoSG Fr1.

## **2.4 Polyacrylamide gel electrophoresis (PAGE)**

PAGE was used to determine the electrophoretic mobility of BoSG Fr1 along with known MWs: low molecular weight heparin (LMWH), unfractionated heparin (UFH), chondroitin sulfate A (CS-A), and chondroitin sulfate C (CS-C). The PAGE system was 1 mm thick and discontinuous. 4% stacking gel and 12% resolving gel phase were prepared. An 8-tooth, well forming comb was utilized to create the wells. During electrophoresis, the comb was removed and 10 µg of BoSG Fr1 and standards of known MWs experienced 100 V. Running electrophoresis used tris buffer (0.5 M, pH 6.8). The movement of bands was surveyed by 0.02% bromocresol green dye that was incorporated into the same gel. The gel was stained with 0.1% (w/v) toluidine blue dissolved in 1% acetic acid after electrophoresis. Destaining of the gel followed multiple washings with 1% acetic acid.

## **2.5 Chemical modifications of BoSG**

### **2.5.1 Desulfation of BoSG Fr1**

The following procedure was performed as specified by previous publication [5]. Chemical desulfation of BoSG Fr1 began with dissolving 5 mg of BoSG Fr1 in 0.5 mL of

distilled water. This solution was then entered into a Dowex 50-W (H<sup>+</sup> 200-400 mesh) column. After subjection of the solution to the column, the fractions with sugar components were gathered and neutralized with pyridine. After neutralization, lyophilization ensued. The resulting pyridinium salt was dissolved in 0.5 mL dimethyl sulfoxide (DMSO)/methanol (9:1 v/v) and heated at 80 °C for 6 h. The resulting product was dialyzed against distilled water and lyophilized again to produce 3.0 mg of desulfated BoSG Fr1.

### **2.5.2 Oversulfation of BoSG Fr1**

Oversulfation of BoSG Fr1 was performed following the procedure from a previous publication [5]. Chemical oversulfation of BoSG Fr1 began with dissolving 5 mg of BoSG Fr1 in 0.5 mL of distilled water. This solution was then entered into a Dowex 50-W (H<sup>+</sup> 200-400 mesh) column. After identifications of designated fractions through metachromasy 1,9-dimethylmethylene blue test, the fractions were pooled and 10% tributylamine in ethanol solution was added. The resulting product was dialyzed against distilled water and lyophilized. The salt produced was dissolved in N,N-dimethylformamide (0.5 mL), and pyridine-stirred for 1 h at 80 °C with the reaction being stopped with the addition of 1.6 mL of distilled water. This product was diluted with three volumes of ethanol which had been saturated with anhydrous sodium acetate. To precipitate, this solution was incubated at 20 °C for 1 h. After centrifugation at 3000 rpm x 30 min the precipitate was collected. The collected precipitate was combined with distilled water, dialysis, and lyophilized to yield the oversulfated BoSG Fr1.

### **2.5.3 Alkaline treatment of BoSG Fr1**

The alkaline treatment procedure followed protocol established in a previously reported procedure [5]. Chemical alkaline treatment of BoSG Fr1 began with 5.0 mg of BoSG Fr1 dissolved in 5% sodium hydroxide (NaOH) solution. After dissolving, the mixture was heated at

80 °C for 3 h. After the reaction took place, the product was dialyzed and lyophilized to yield 2.8 mg of the alkali-treated BoSG Fr1.

### **3. Results and Discussion**

#### **3.1 Structure characterization of BoSG**

##### **3.1.1 Isolation and preliminary physiochemical analyses of BoSG Fr1**

Using papainolytic digestion of the dried cell wall of the red alga *B. occidentalis*, the major sulfated polysaccharides, BoSGs, were isolated. Subsequent purification using anion-exchange chromatography on the DEAE sephacel column indicated the presence of three specific BoSG populations of distinct polyanionic compositions. This purification was performed linearly with a 1-3 M NaCl gradient (Figure 2). 1,9-dimethylmethylene blue (DMB) tests were used to identify the polysaccharide fractions after the column by metachromasy (absorbance at 525 nm). The chromatograph illustrates three peaks of interest from *B. occidentalis*: the first, labeled Fr1, and two other peaks, labeled Fr2 and Fr3. Following elution time, it is assumed Fr1 has the lowest sulfation content while the other two peaks follow a pattern of greater sulfation as extraction occurred. Specifically, these three peaks were eluted from the anion-exchange column at NaCl concentrations of 0.5, 1.2, and 1.5 M (Figure 2). The unexplored Fr1 of BoSG was subject to various processes for analysis of MW, polydispersity, full structural characterization, and binding properties to blood co-factors.

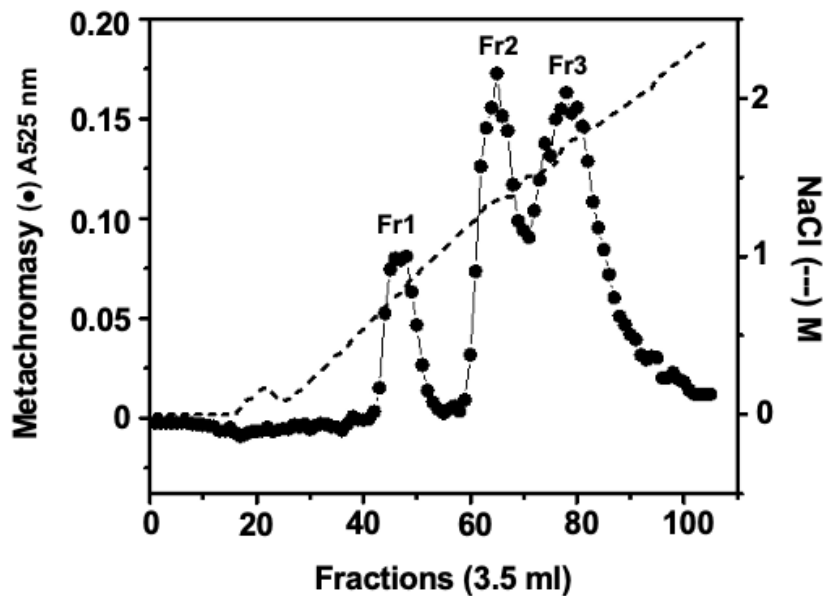


Figure 2. Fractionation of BoSG

To determine the MW of Fr1 of BoSG, HPSEC/MALS as well as PAGE analysis was employed. Figure 3 depicts that BoSG Fr 1 has a MW of  $70.24 \pm 2.144$  kDa. PAGE offers to compare the molecular dispersity of BoSG Fr 1 against other common sulfated glycans like LMWH (~8kDa), UFH (~15 kDa), CS-A (~40 kDa), and CS-C (~60 kDa). Through electrophoretic migration, BoSG Fr1 illustrated a polydisperse material with multiple chains consisting of MWs within 20 to  $\geq 100$ kDa (Figure 4). The correlation between the HSPEC/MALS profile and the PAGE analysis indicates an accurate assessment of the MW of BoSG Fr1.

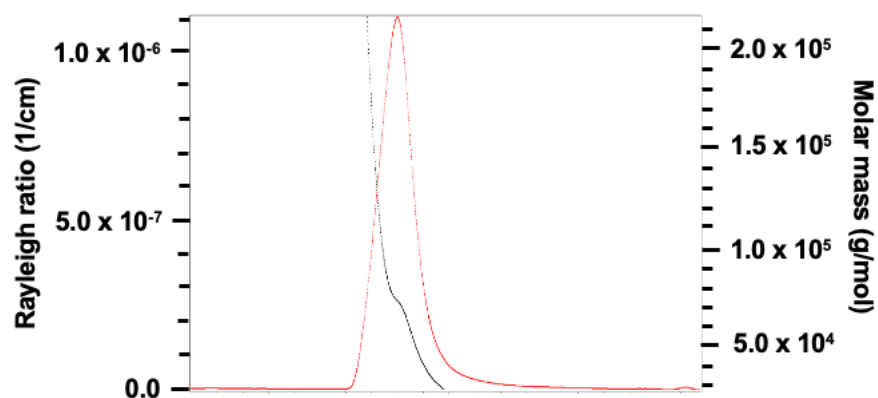


Figure 3. HPSEC-MALS profile of BoSG Fr1

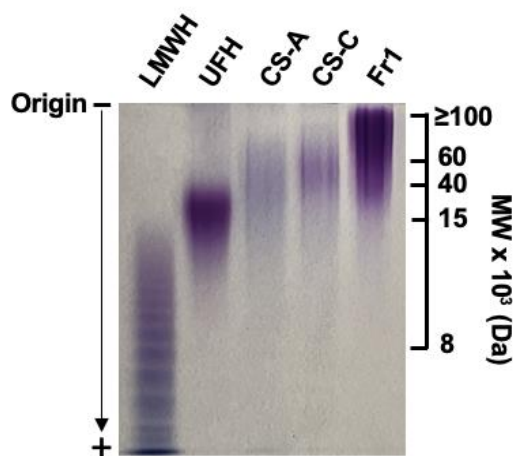
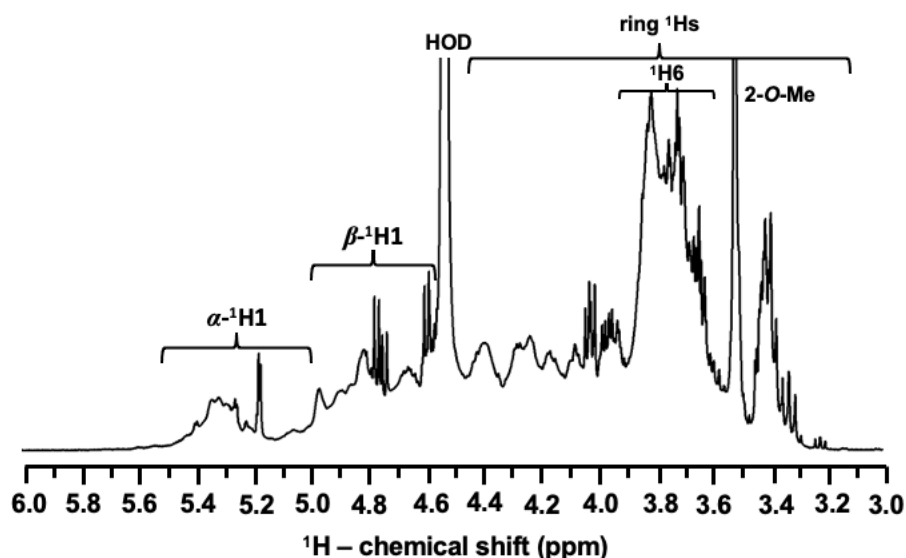


Figure 4. PAGE MW analysis of BoSG Fr1

### 3.1.2 NMR spectroscopy

The structural characterization of BoSG and the specific Gal units composing Fr1 were achieved by a combination of 1D and multiple 2D NMR techniques. Characteristic of SGs, the 1D  $^1\text{H}$  NMR spectrum of Fr1 (Figure 5) indicated two anomeric signals ( $^1\text{H}_1$ ). One of the sets coordinates with the  $\alpha$ -Gal units while the other coordinates with the  $\beta$ -Gal units of Fr1. The  $\alpha$ -

Gal residues are characterized by the most downfield anomeric  $^1\text{H1}$  resonances of the spectrum ( $\delta_{\text{H}}$  between 5.6 and 5.0 ppm), while the  $\beta$ -Gal are characterized by the most upfield anomeric  $^1\text{H1}$  resonances of the spectrum ( $\delta_{\text{H}}$  between 5.0 and 4.6 ppm). Other important features of the  $^1\text{H}$  NMR spectra include the  $^1\text{H}$  signals of the ring  $^1\text{Hs}$  ( $\delta_{\text{H}}$  between 4.5 and 3.2 ppm), the  $\text{CH}_2$  chemical groups outside of the hexose ring ( $\delta_{\text{H}}$  between 3.9 and 3.6 ppm), and  $\text{CH}_3$  ( $\delta_{\text{H}}$  around 3.5 ppm). These groups are evaluated with greater detail in the 2D NMR spectra.



**Figure 5.** 1D  $^1\text{H}$  NMR spectrum of BoSG Fr1 ( $\delta_{\text{H}}$  expansion from 6.0 to 3.0 ppm)

The following 2D NMR spectra were utilized to determine the structure of the Gal units of BoSG Fr1:  $^1\text{H}/^1\text{H}$  COSY for short-range carbon-bonded vicinal/geminal  $^1\text{Hs}$  (Figure 6A),  $^1\text{H}/^1\text{H}$  TOCSY for long-range carbon-bonded  $^1\text{H}$  spins (Figure 6B), and  $^1\text{H}/^{13}\text{C}$ -edited HSQC for proton-carbon pairs (Figure 6C). Figures 6A, and 6B include the anomeric  $^1\text{H}$  region of COSY and TOCSY spectra. All Gal units of BoSG Fr1 (Table 1) were obtained with all  $^1\text{H}$  chemical shifts ( $\delta_{\text{H}}$ ) from the COSY and TOCSY spectra and  $^{13}\text{C}$  shifts from the HSQC spectrum. The  $\delta_{\text{H}}$

and  $\delta_C$  within the hexose rings of the specific Gal units of BoSG Fr1 were labeled in Table 1 with a system of letters (A to N) followed by numbers (1 to 6). With consideration of the  $\delta_H$  shift ( $\sim 0.6$  ppm), downfield  $\delta_C$  shift ( $\sim 6$  ppm) of sulfation (bold values) and glycosylation (italic values), the identified sulfation patterns and glycosidic bonds in the Gal units of BoSG Fr1 using  $\delta_H$  and  $\delta_C$  values were possible when compared to previous literature [5,14-20] (Table 1). The presence of 3,6-anhydro Gal moiety in the  $\alpha$ -AnGal units and methylation were apparent when analyzing the  $\delta_H$  and  $\delta_C$  values of other ring positions.

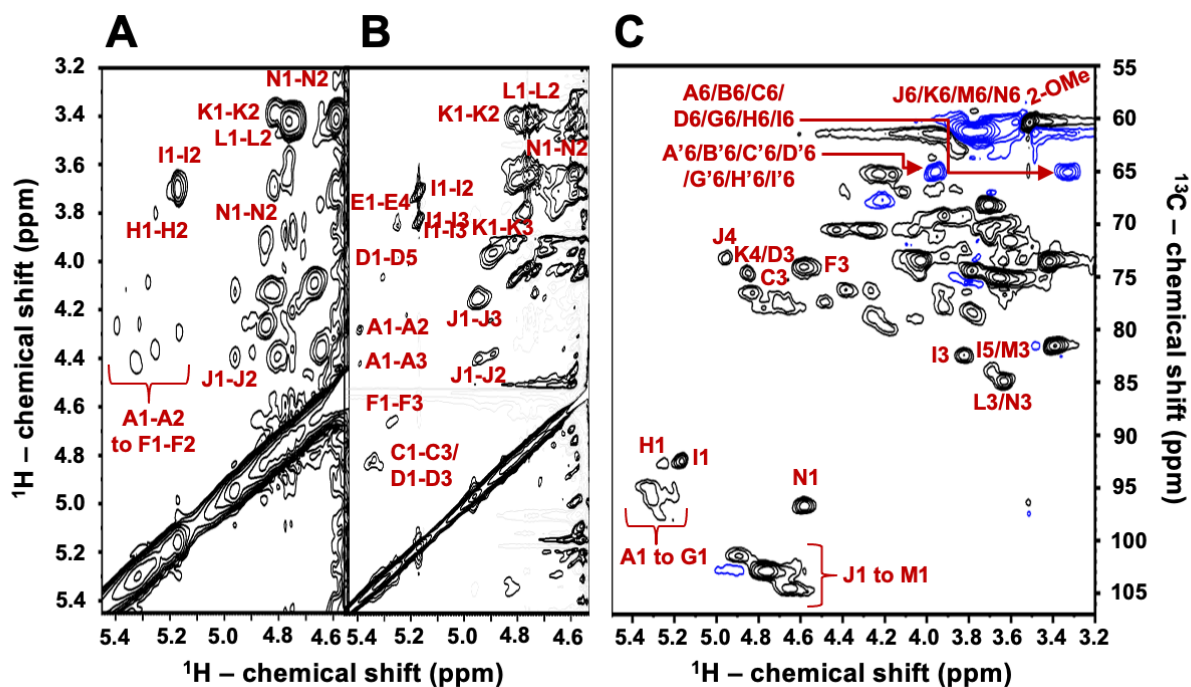


Figure 6. (A) 2D  $^1\text{H}/^1\text{H}$  COSY and (B)  $^1\text{H}/^1\text{H}$  TOCSY, and (C)  $^1\text{H}/^{13}\text{C}$ -edited HSQC NMR spectra of native BoSG Fr1.

**Table 1.** <sup>1</sup>H and <sup>13</sup>C chemical shifts (ppm) of the composing units from BoSG Fr1 and from references. Values in bold indicate sulfation sites while values in italic indicate glycosylation sites.

| Unit: [structure] and (letter notation)        | Source | <sup>1</sup> H1/ <sup>13</sup> C1 | <sup>1</sup> H2/ <sup>13</sup> C2 | <sup>1</sup> H3/ <sup>13</sup> C3 | <sup>1</sup> H4/ <sup>13</sup> C4 | <sup>1</sup> H5/ <sup>13</sup> C5 | <sup>1</sup> H6/ <sup>13</sup> C6 | 2-O-Me    |
|--|--------|-----------------------------------|-----------------------------------|-----------------------------------|-----------------------------------|-----------------------------------|-----------------------------------|-----------|
| [→4)-α-AnGal-2-(SO3 <sup>-</sup> )-(1→) (A1)   | Fr1    | 5.39/94.8                         | <b>4.27/78.7</b>                  | 4.41/76.1                         | <i>4.16/79.7</i>                  | 4.03/74.0                         | 3.32, 3.94/64.9                   | -         |
| [→4)-α-AnGal-2-(SO3 <sup>-</sup> )-(1→)        | [5]    | 5.35/94.7                         | <b>4.40/76.7</b>                  | 4.81/78.7                         | -                                 | -                                 | -                                 | -         |
| [→4)-α-AnGal-2-O-Me-(1→) b (B1)                | Fr1    | 5.35/96.0                         | 4.09/79.2                         | 4.24/78.9                         | 3.83/78.5                         | 3.74/76.1                         | 3.32, 3.94/64.9                   | 3.51/60.1 |
| [→4)-α-AnGal-2-O-Me-(1→)                       | [14]   | 5.31/98.7                         | 3.55/78.8                         | 3.85/78.4                         | <i>3.65/77.6</i>                  | 3.45/75.3                         | 3.33/69.8                         | 3.51/60.1 |
| [→4)-α-AnGal-2-(SO3 <sup>-</sup> )-(1→) (C1)   | Fr1    | 5.32/95.4                         | <b>4.41/76.1</b>                  | 4.81/77.3                         | <i>4.16/79.7</i>                  | 4.05/74.0                         | 3.32, 3.94/64.9                   | -         |
| [→4)-α-AnGal-2-(SO3 <sup>-</sup> )-(1→)        | [5]    | 5.35/94.7                         | <b>4.40/76.7</b>                  | 4.81/78.7                         | -                                 | -                                 | -                                 | -         |
| [→4)-α-AnGal-(1→) (D1)                         | Fr1    | 5.31/95.6                         | 4.26/70.6                         | 4.87/74.4                         | 3.83/78.5                         | 4.29/78.9                         | 3.32, 3.94/64.9                   | -         |
| [→4)-α-AnGal-(1→)                              | [15]   | 5.07/94.7                         | 4.08/70.4                         | 4.53/79.7                         | <i>4.60/78.5</i>                  | 4.67/77.1                         | 3.32, 3.94/64.9                   | -         |
| [→4)-α-AnGal-2-O-Me-(1→) (E1)                  | Fr1    | 5.27/97.0                         | 4.09/78.7                         | 4.22/78.9                         | 3.83/78.5                         | 3.74/76.1                         | 3.32, 3.94/64.9                   | 3.51/60.1 |
| [→4)-α-AnGal-2-O-Me-(1→)                       | [16]   | 5.31/98.7                         | 3.55/78.8                         | 3.85/78.4                         | <i>3.65/77.6</i>                  | 3.45/75.3                         | 3.33/69.8                         | 3.51/60.1 |
| [→4)-α-AnGal-2-(SO3 <sup>-</sup> )-(1→) (F1)   | Fr1    | 5.25/95.4                         | <b>4.36/76.1</b>                  | 4.64/74.3                         | <i>3.98/78.7</i>                  | -                                 | -                                 | -         |
| [→4)-α-AnGal-2-(SO3 <sup>-</sup> )-(1→)        | [16]   | 5.27/94.7                         | <b>4.66/75.4</b>                  | 4.78/78.1                         | <i>4.72/78.3</i>                  | 4.70/78.1                         | 4.06, 4.21/70.0                   | -         |
| [→4)-α-AnGal-2-(SO3 <sup>-</sup> )-(1→) (G1)   | Fr1    | 5.16/95.6                         | <b>4.29/78.5</b>                  | 4.41/76.1                         | <i>4.13/79.0</i>                  | 3.96/77.5                         | 3.32, 3.94/64.9                   | -         |
| [→4)-α-AnGal-2-(SO3 <sup>-</sup> )-(1→)        | [16]   | 5.27/94.7                         | <b>4.66/75.4</b>                  | 4.78/78.1                         | <i>4.72/78.3</i>                  | 4.70/78.1                         | 4.06, 4.21/70.0                   | -         |
| [→4)-α-AnGal-(1→) (H1)                         | Fr1    | 5.25/92.5                         | 3.79/70.0                         | 4.33/76.2                         | <i>4.02/79.2</i>                  | 4.21/79.0                         | 3.32, 3.94/64.9                   | -         |
| [→4)-α-AnGal-(1→)                              | [15]   | 5.07/94.7                         | 4.08/70.4                         | 4.53/79.7                         | <i>4.60/78.5</i>                  | 4.67/77.1                         | 3.32, 3.94/64.9                   | -         |
| [→4)-α-AnGal-(1→) (I1)                         | Fr1    | 5.17/92.3                         | 3.69/71.1                         | 3.82/82.3                         | <i>4.05/79.2</i>                  | 3.70/83.6                         | 3.32, 3.94/64.9                   | -         |
| [→4)-α-AnGal-(1→)                              | [15]   | 5.07/94.7                         | 4.08/70.4                         | 4.53/79.7                         | <i>4.60/78.5</i>                  | 4.67/77.1                         | 3.32, 3.94/64.9                   | -         |
| [→3)-β-D-Gal-2,4-(SO3 <sup>-</sup> )-(1→) (J1) | Fr1    | 4.94/101.4                        | <b>4.39/76.1</b>                  | <i>4.15/79.7</i>                  | <b>4.97/73.5</b>                  | 3.95/69.6                         | 3.70/61.1                         | -         |
| [→3)-β-D-Gal-2,4-(SO3 <sup>-</sup> )-(1→)      | [13]   | 4.94/102.4                        | <b>4.41/76.7</b>                  | <i>4.18/81.1</i>                  | <b>4.99/74.2</b>                  | -                                 | 3.77/62.4                         | -         |
| [→3)-β-D-Gal-4-(SO3 <sup>-</sup> )-(1→) (K1)   | Fr1    | 4.80/102.8                        | 3.37/73.2                         | <i>4.02/79.2</i>                  | <b>4.88/74.4</b>                  | 3.82/74.4                         | 3.70/61.1                         | -         |
| [→3)-β-D-Gal-4-(SO3 <sup>-</sup> )-(1→)        | [16]   | 4.70/102.5                        | 3.65/69.4                         | <i>4.06/78.2</i>                  | <b>4.91/73.7</b>                  | 3.87/74.8                         | 3.86/61.2                         | -         |
| [→3)-β-D-Gal-(1→) (L1)                         | Fr1    | 4.75/102.0                        | 3.43/73.7                         | <i>3.62/84.9</i>                  | 4.01/70.0                         | 3.38/73.5                         | -                                 | -         |
| [→3)-β-D-Gal-(1→)                              | [18]   | 4.79/103.5                        | 3.90/69.9                         | <i>3.93/81.9</i>                  | 4.29/68.3                         | 3.82/74.8                         | 3.87/60.5                         | -         |
| [→3)-β-D-Gal-(1→) (M1)                         | Fr1    | 4.65/103.7                        | 4.08/73.2                         | 3.71/83.9                         | 4.02/70.1                         | 3.38/73.2                         | 3.62/61.1                         | -         |
| [→3)-β-D-Gal-(1→)                              | [19]   | 4.57/104.5                        | 3.63/72.1                         | <i>3.73/84.1</i>                  | 4.12/71.4                         | 3.76/73.7                         | 3.77/63.4                         | -         |
| [→3)-β-D-Gal-(1→) (N1)                         | Fr1    | 4.58/97.0                         | 3.42/73.7                         | <i>3.65/85.0</i>                  | 4.01/70.1                         | 3.37/73.5                         | 3.61/61.3                         | -         |

The α-AnGal sulfation patterns (A, C, F, and G) were indicated at ring position 2 with downfield δ<sub>H</sub>-δ<sub>C</sub> (δ<sub>H</sub>/δ<sub>C</sub> at 4.27/78.7, 4.41/76.1, 4.36/76.1, and 4.29/78.5 ppm, respectively) (Table 1). The downfield δ<sub>H</sub>-δ<sub>C</sub> illustrated the α-AnGal residues contained 2-O-sulfation. Attached to the ring position 2 in α-AnGal residues B and E in Table 1, the δ<sub>H</sub>/δ<sub>C</sub> pair of 3.51/60.1 ppm in all 2D spectra indicates a methoxy group (O-CH<sub>3</sub>) not including the ring atoms

$^1\text{H}1/^1\text{H}6$  and  $^{13}\text{C}1/^13\text{C}6$ . Due to no downfield chemical shifts of the ring  $^1\text{H}$  and  $^{13}\text{C}$  nuclei, B, D, E, H, and I  $\alpha$ -AnGal received non-sulfated designation (Table 1).  $\beta$ -Gal units with expected downfield shifts of  $\delta_{\text{H}}/\delta_{\text{C}}$  at  $\sim 4.4/76$  ppm and  $\delta_{\text{H}}/\delta_{\text{C}}$  at  $\sim 4.9/74$  ppm labeled J and K are characteristic of 2-O- and 4-O-sulfation (Table 1). Labeled  $\beta$ -Gal units, L, M, and N, were characterized as non-sulfated with lack of chemical shifts downfield in their ring nuclei ( $^1\text{H}$  and  $^{13}\text{C}$ ) in Table 1. 40:60% was the calculated relative integrals of the NMR signals for sulfated:non-sulfated Gal units in BoSG Fr1.

Utilizing chemical modification of BoSG Fr1, confirmation of the  $^1\text{H}/^{13}\text{C}$  NMR spectral designations of sulfation and 3,6-anhydro moiety of the Gal units were accomplished. Specifically, desulfated, oversulfated, and alkali-treated (AnGal-enriched) samples of BoSG Fr1 were used as chemical modifications. As predicted, the sulfated sites with  $\delta_{\text{H}}/\delta_{\text{C}}$  range of 5.0-4.4/80-70 ppm were removed in the HSQC spectrum of the desulfated derivative after the process of desulfation (Figure 7A). This effect was coupled with increased intensity of negative-phased resonances L6/M6 with  $\delta_{\text{H}}/\delta_{\text{C}}$  at  $\sim 3.7/60$  ppm and the reduction of sulfated cross-peaks  $^1\text{H}6/^13\text{C}6$  cross-peaks with  $\delta_{\text{C}}$  at 65 ppm (Figure 7A). The HSQC oversulfated spectrum shows increased intensity of negative-phased, blue-counteracted peaks with  $\delta_{\text{H}}/\delta_{\text{C}}$  around 4.25/67 ppm, and the black-counteracted peaks with  $\delta_{\text{H}}/\delta_{\text{C}}$  range of 5.0-4.4/80-70 ppm which are all sulfate related  $^1\text{H}/^{13}\text{C}$  cross-peaks (Figure 7B).  $^1\text{H}/^{13}\text{C}$  HSQC spectra with alkali treatment confirmed the presence of  $\alpha$ -AnGal units in BoSG Fr1 when compared to the HSQC of the native (Figure 7C).  $\text{CH}_2$  negative-phased  $^1\text{H}/^{13}\text{C}$  cross-peaks illustrated similar signal intensities. This confirms that  $\alpha$ -Gal units appear mainly as 3,6-anhydro units in BoSG Fr1. Figure 8 depicts the structures

of all Gal units of BoSG Fr1 that were characterized from the native 1D and 2D NMR spectra as well as comparisons to the spectra of chemical derivatives of BoSG Fr1.

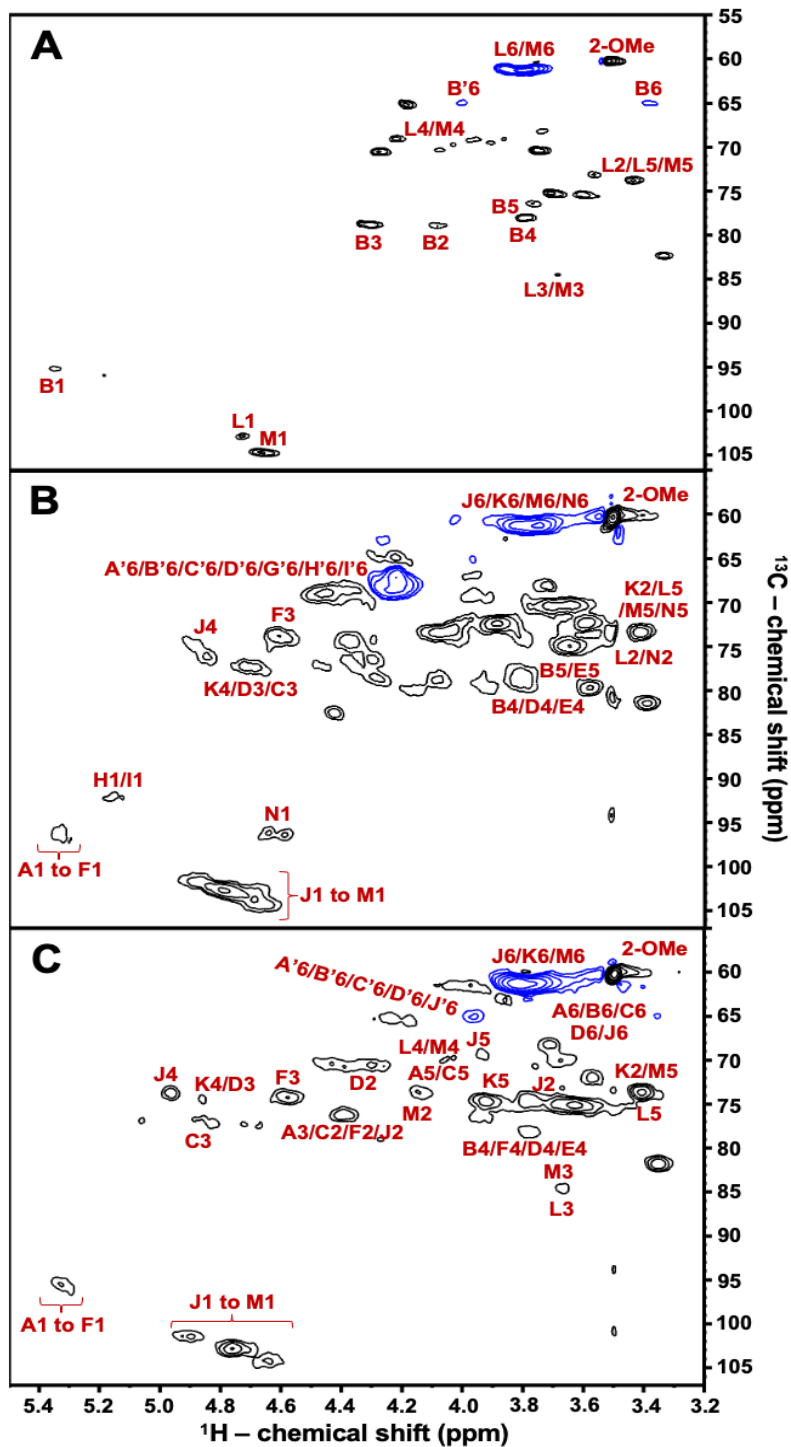


**Figure 7.** 2D  $^1\text{H}/^{13}\text{C}$  HSQC NMR spectra of chemical modified BoSG Fr1: (A) desulfated, (B) oversulfated, and (C) alkali-treated AnGal-enriched derivatives

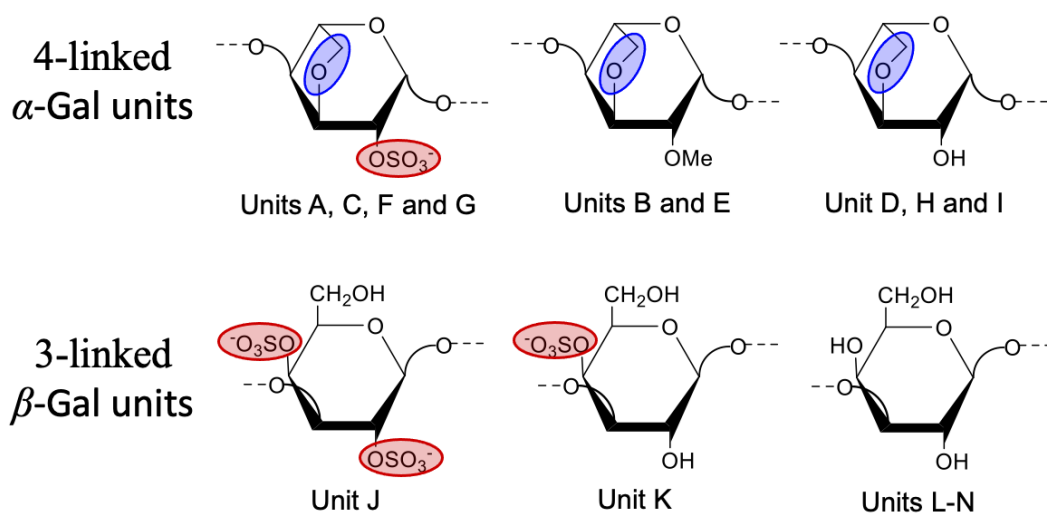


**Figure 8.** Structural illustration of BoSG Fr1 as identified by NMR analyses. The backbone of BoSG identifies as 4-linked  $\alpha$  and 3-linked  $\beta$  glycosidic linkages. Chemical modifications of BoSG include sulfation at different positions as well as 3,6-anhydro moiety and methylation at the 2-O position. The red ellipses represent sulfation esters while the 3,6-anhydro moiety is highlighted with the blue ellipses. Letters listed in NMR assignments coordinate with the indicated structures.

## 3.2 Binding properties of BoSG Fr1

### 3.2.1 SPR spectroscopy

In this study, BoSG Fr-1-derived samples from the NMR-based analyses (native, desulfated, oversulfated, and alkali-treated) and the four main blood co-factors (IIa, Xa, AT, and HCII) were evaluated in inhibitory percentage of the binding of each of the co-factors alone (Figure 9). UFH, the standard mammalian glycosaminoglycan of high anticoagulant activity, was utilized as a positive control. The native BoSG Fr1 showed stronger inhibition of HCII than UFH (100% BoSG Fr1 vs 65% UFH) but showed weaker inhibition of IIa (40% BoSG Fr1 vs 70% UFH), Xa (35% BoSG Fr1 vs 85% UFH), and AT (25% BoSG Fr1 vs 100% UFH) than UFH (Figure 9). Against the heparin sensor chip, the binding inhibitory property of BoSG Fr1 to the main co-factors could follow the observed order HCII > IIa = Xa >> AT. This experiment proves

the strong preference of BoSG Fr1 to blood co-factor HCII as well as the weaker binding property of UFH to HCII in comparison to BoSG Fr1. Also, the need to use a higher concentration of HCII (800 nM) to observe interaction with the heparin surface during the SPR analysis enforces the previously stated weak interaction between HCII and the heparin as compared to the other co-factors.

As previously stated about the importance of sulfation in biological activity, the binding inhibition was severely decreased by the desulfation (deS) of BoSG Fr1. However, this was not observed in AT binding where the binding inhibition did not vary from the native. The reverse side of this concept did not hold true with oversulfation (overS). The binding inhibition of native BoSG could not be enhanced by oversulfation due to no change in the results of binding inhibition with the overS derivative as compared to the native. The lack of change in binding inhibition was also observed in the alkali-treated (Alk) derivative which indicates that this chemical modification does not have an effect on the binding of BoSG Fr1 to the blood co-factors.

The least sulfated unit, Fr1 of BoSG, displays relative weak binding inhibition to the four blood co-factors. This idea can be mainly inferred from the structure of this BoSG derivative that contains significant AnGal units and O-methylation. Also, the low sulfation of this BoSG fraction (40% of all Gal units) can also be attributed to its weak binding properties. AnGal units have been previously proven to decrease coagulation binding in proteases (IIa and Xa) and serpins (AT and HCII). When negatively charged sulfate groups in sulfated polysaccharides in cohorts with positively charged amino acids contribute to the overall binding quality, methylation of these species does not enhance interaction of sulfated polysaccharides to binding proteins.

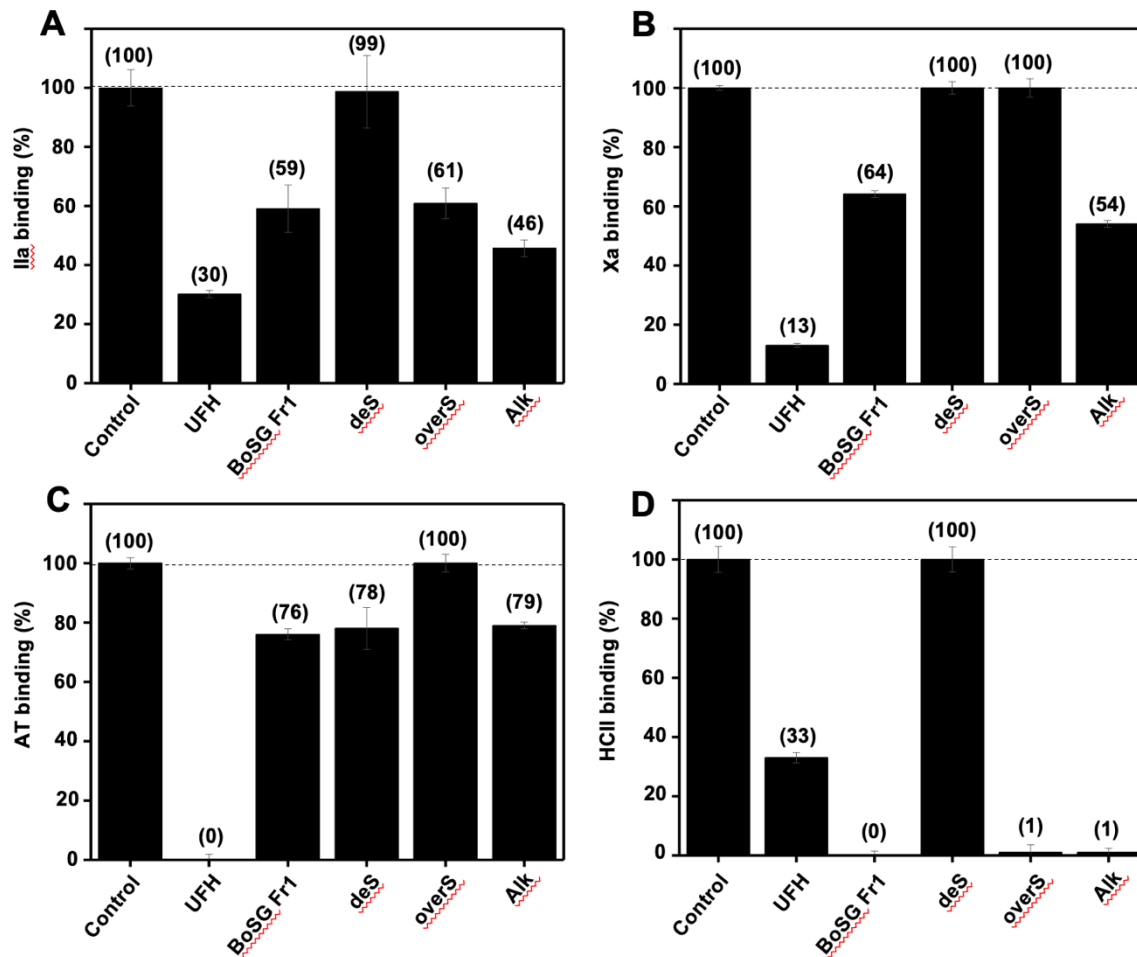


**Figure 9.** Solution SPR competitive effect of native BoSG Fr1 and its chemical derivatives on binding of blood co-factors to heparin surface: (A) IIa, (B) Xa, (C) AT, and (D) HCII in the absence of any glycan (negative control), presence of UFH (positive control), BoSG Fr1, and its modifications of desulfation (deS), oversulfation (overS), and alkali-treatment (Alk).

#### 4. Conclusions

BoSG Fr1 is a distinct sulfated polysaccharide found within the cell wall of the red alga *B. occidentalis*, isolated from the total anionic polysaccharides, when subjected to anion-exchange chromatography. In a recent publication, the revised structure of the other distinct fractions was reported (BoSG Fr2 and Fr3) [5]. The structure of the first BoSG fraction (Fr1), the initial peak from the anion-exchange chromatography, was examined here for the first time which follows the pattern of backbones being composed of both 4-linked  $\alpha$ - and 3-linked  $\beta$ -Gal

units. Our reports indicate that BoSG Fr1 contains significant amounts (60% of total Gal units) of non-sulfated Gal units, alongside substantial quantities of 2-O-methylated or 2-O-sulfated  $\alpha$ -AnGal units, and 4-O-sulfated or 2,4-di-O-sulfated  $\beta$ -Gal units. The molecular weight of 70 kDa for BoSG Fr1 is comparable to the other fractions. Regarding biological activity, weaker interactions of BoSG Fr 1 were observed as compared to UFH for IIa, Xa, and AT; however, binding of BoSG Fr1 is greater in HCII than the positive control. The mediocre biomedical properties of BoSG result from the balance between a lack of sulfation (half of total backbone Gal units) and the presence of other chemical modifications like the 3,6-anhydro moiety and methylation which result lower binding affinity to blood co-factors. In summary, this report, coupled with our previous research, concludes both the structural characterization of all three BoSGs and the correlation between their composing structural features and their levels of binding to the four key blood co-factors.

## REFERENCES

1. Singh, H., Parida, A., Debbarma, K., Ray, D. P., & Banerjee, P. (2020). Common marine organisms: a novel source of medicinal compounds. *International Journal of Bioresource Science*, 7(2), 39-49.
2. Jiao, G., Yu, G., Zhang, J., & Ewart, H. S. (2011). Chemical structures and bioactivities of sulfated polysaccharides from marine algae. *Marine drugs*, 9(2), 196-223.
3. Pereira, M. S., Melo, F. R., & Mourão, P. A. (2002). Is there a correlation between structure and anticoagulant action of sulfated galactans and sulfated fucans?. *Glycobiology*, 12(10), 573-580.
4. Farias, W. R. L., Valente, A. P., Pereira, M. S., & Mourão, P.A.S. (2000). Structure and Anticoagulant Activity of Sulfated Galactans. Isolation of a unique sulfated galactan from the red algae *Botryocladia occidentalis* and comparison of its anticoagulant action with that of sulfated galactans from invertebrates. *Journal of Biological Chemistry*, 275, 29299-29307
5. Maurya, A.K.; Sharma, P.; Samanta, P.; Shami, A.A.; Misra, S.K.; Zhang, F.; Thara, R.; Kumar, D.; Shi, D.; Linhardt, R.J.; Sharp, J.S.; Doerksen, R.J.; Tandon, R.; Pomin, V.H. Structure, anti-SARS-CoV-2, and anticoagulant effects of two sulfated galactans from the red alga *Botryocladia occidentalis*. *International Journal of Biological Macromolecules*, 2023, 238, 124168.
6. Costa, L. S., Fidelis, G. P., Cordeiro, S. L., Oliveira, R. M., Sabry, D. A., Câmara, R. B. G., ... & Rocha, H. A. O. (2010). Biological activities of sulfated polysaccharides from tropical seaweeds. *Biomedicine & Pharmacotherapy*, 64(1), 21-28.
7. Wang, J. Q., Yin, J. Y., Nie, S. P., & Xie, M. Y. (2021). A review of NMR analysis in polysaccharide structure and conformation: Progress, challenge and perspective. *Food Research International*, 143, 110290.
8. Kwan, A. H., Mobli, M., Gooley, P. R., King, G. F., & Mackay, J. P. (2011). Macromolecular NMR spectroscopy for the non-spectroscopist. *The FEBS journal*, 278(5), 687-703.
9. Reif, B., Ashbrook, S. E., Emsley, L., & Hong, M. (2021). Solid-state NMR spectroscopy. *Nature Reviews Methods Primers*, 1(1), 2.

10. Jameson, C. J. (1996). Understanding NMR chemical shifts. *Annual review of physical chemistry*, 47(1), 135-169.
11. Yu, H., Munoz, E. M., Edens, R. E., & Linhardt, R. J. (2005). Kinetic studies on the interactions of heparin and complement proteins using surface plasmon resonance. *Biochimica et Biophysica Acta (BBA)-General Subjects*, 1726(2), 168-176.
12. Castillo, J., Gutierrez, H., Chirinos, J., & Perez, J. C. (2010). Surface plasmon resonance device with imaging processing detector for refractive index measurements. *Optics Communications*, 283(20), 3926-3930.
13. Sparks, R. P., Jenkins, J. L., & Fratti, R. (2019). Use of surface plasmon resonance (SPR) to determine binding affinities and kinetic parameters between components important in fusion machinery. *SNAREs: Methods and Protocols*, 199-210.
14. Gong, G.; Zhao, J.; Wang, C.; Wei, M.; Dang, T.; Deng, Y.; Sun, J.; Song, S.; Huang, L.; Wang, Z. Structural characterization and antioxidant activities of the degradation products from *Porphyra haitanensis* polysaccharides. *Process Biochemistry* 2018, 74, 185-193.
15. Sanchez, R.A.R.; Matulewicz, M.C.; Ciancia, M. NMR spectroscopy for structural elucidation of sulfated polysaccharides from red seaweeds. *International Journal of Biological Macromolecules*. 2022, 199, 386-400.
16. Albano, R.M.; Pavão, M.S.G.; Mourão, P.A.S.; Mulloy, B. Structural studies of a sulfated L-galactan from *Styela plicata* (Tunicate): analysis of the smith-degraded polysaccharide. *Carbohydrate Research*, 1990, 208, 163-174.
17. Vasconcelos, A.A.; Pomin, V.H. The sea as a rich source of structurally unique glycosaminoglycans and mimetics. *Microorganisms*, 2017, 5, 51.
18. Castro, M.O.; Pomin, V.H.; Santos, L.L.; Vilela-Silva, A.E.S.; Hirohashi, N.; Pol-Fachin, L.; Verli, H.; Mourão, P.A.S. A unique 2-sulfated  $\beta$ -galactan from the egg jelly of the sea urchin *Glyptocidaris crenularis*: Confirmation flexibility versus induction of the sperm acrosome reaction. *Journal of biological chemistry*, 2009, 284, 18790- 18800.
19. Pereira, M.G.; Benevides, N.M.B.; Melo, M.R.S.; Valente, A.P.; Melo, F.R.; Mourão, P.A.S. Structure and anticoagulant activity of a sulfated galactan from the red alga, *Gelidium crinale*. Is there a specific structural requirement for the anticoagulant action? *Carbohydrate Research*. 2005, 340, 2015-2023.

20. Maurya, A. K., Ahmed, H. A., DeWitt, A., Shami, A. A., Misra, S. K., & Pomin, V. H. (2024). Structure and Binding Properties to Blood Co-Factors of the Least Sulfated Galactan Found in the Cell Wall of the Red Alga *Botryocladia occidentalis*. *Marine Drugs*, 22(2), 81.